

E+A and Companion Galaxies - I : A Catalogue and Statistics

Chisato Yamauchi^{1,2}, Masafumi Yagi² and Tomotsugu Goto^{2,3}

¹*Institute of Space and Astronautical Science, Japan Aerospace Exploration Agency, 3-1-1 Yoshinodai, Sagami-hara, Kanagawa, 229-8510, Japan*

²*National Astronomical Observatory, 2-21-1 Osawa, Mitaka, Tokyo 181-8588, Japan*

³*Institute for Astronomy, University of Hawaii 2680 Woodlawn Drive, Honolulu, HI, 96822, USA*

11 August 2024

ABSTRACT

Based on our intensive spectroscopic campaign with the GoldCam spectrograph on the Kitt Peak National Observatory (KPNO) 2.1-m telescope, we have constructed the first catalogue of E+A galaxies with spectroscopic companion galaxies, and investigated a probability that an E+A galaxy have close companion galaxies. We selected 660 E+A galaxies with $40\text{\AA} < H - EW$ at a redshift of < 0.167 from the Data Release 5 of the Sloan Digital Sky Survey (SDSS). We selected their companion candidates from the SDSS imaging data, and classified them into true companions, fore/background galaxies and companion candidates using the SDSS and our KPNO spectra. We observed 26 companion candidates of E+A galaxies at the KPNO to measure their redshifts. Their spectra showed that 17 targets are true companion galaxies. The number of spectroscopically-confirmed E+A's companions are now 34. This becomes the first catalogue of E+A galaxies with spectroscopic companion systems. We found that E+A galaxies have an 54% larger probability of having companion galaxies (7.88%) compared to the comparison sample of normal galaxies (5.12%). A statistical test shows the probabilities are different with 99.7% significance. Our results based on spectroscopy tightens the connection between the dynamical merger/interaction and the origin of E+A galaxies.

Key words: galaxies: evolution, galaxies:interactions, galaxies:starburst, galaxies:peculiar

1 INTRODUCTION

Dressler & Gunn (1983, 1992) discovered galaxies with mysterious spectra in high-redshift clusters of galaxies. These galaxies had strong Balmer absorption lines with no emission in $[O III]$. They were named “E+A” galaxies because their spectra resembled a superposition of those of elliptical galaxies (Mg₅₁₇₅, Fe₅₂₇₀ and Ca_{3934;3468} absorption lines) and A-type stars (Strong Balmer absorption)¹. The existence of strong Balmer absorption lines shows that these galaxies have experienced starbursts within the last Gyr, since the lifetime of an A-type star is about 1 Gyr. However, they show no sign of ongoing star formation as indicated by non-detection in the $[O III]$ emission line. Therefore, E+A galaxies are interpreted as post-starburst galaxies, i.e., galaxies that have undergone truncated starburst activity (Dressler & Gunn 1983, 1992; Couch & Sharples 1987;

MacLaren, Ellis & Couch 1988; Newberry, Boroson & Kirshner 1990; Fabricant, McClintock & Bautz 1991; Abraham et al. 1996). Thus, E+A galaxies have attracted a great deal of attention, and some explanations for their origin have been proposed.

In the classical studies, “E+A” galaxies were found in cluster regions in both low-redshift clusters (Franx 1993; Caldwell et al. 1993; Caldwell & Rose 1997; Castander et al. 2001; Rose et al. 2001) and high-redshift clusters (Sharples et al. 1985; Lavery & Henry 1986; Couch & Sharples 1987; Broadhurst, Ellis & Shanks 1988; Fabricant, McClintock & Bautz 1991; Belloni et al. 1995; Barger et al. 1996; Fisher et al. 1998; Morris et al. 1998; Couch et al. 1998; Dressler et al. 1999). Therefore, a cluster-specific phenomenon was thought to be responsible for the violent star formation history of E+A galaxies. A ram-pressure stripping model (Spitzer & Baade 1951; Gunn & Gott 1972; Farouki & Shapiro 1980; Kent 1981; Abadi, Moore & Bower 1999; Fujita & Nagashima 1999; Quilis, Moore & Bower 2000; Fujita 2004; Fujita & Goto 2004) as well as tides from the cluster potential (e.g., Fujita 2004) may first accelerate star formation of cluster of galaxies and later turn it off. However, recent large surveys of the nearby Universe found many E+A galaxies in the field regions (Goto 2003; Goto et al. 2003b; Goto 2005; Blake et al. 2004; Quintero et al. 2004; Hogg et al. 2006). It is obvious that these E+A galaxies in the field regions cannot be explained by a physical mecha-

² E-mail:cyamauch@ir.isas.jaxa.jp

³ Visiting Astronomer, Kitt Peak National Observatory, National Optical Astronomy Observatory, which is operated by the Association of Universities for Research in Astronomy, Inc. (AURA) under cooperative agreement with the National Science Foundation.

¹ Because the spectra of elliptical galaxies are characterised by K stars, these galaxies are sometimes called “k+a” galaxies (e.g., Franx 1993; Dressler et al. 1999; Bartholomew, Rose & Gaba 2001). Following the first discovery, we refer to them as “E+A” throughout this paper.

nism that works in the cluster region. E+A galaxies have often been thought to be transitional objects during cluster galaxy evolution, involving phenomena such as the Butcher-Oemler effect (e.g., Butcher & Oemler 1978; Rakos & Schombert 1995; Margoniner et al. 2001; Ellingson et al. 2001; Kodama & Bower 2001; Goto et al. 2003a), the morphology-density relation (e.g., Dressler 1980; Postman & Geller 1984; Fasano et al. 2000; ?; Postman et al. 2005; Smith et al. 2005), and the correlation between various properties of the galaxies and the environment (e.g., Tanaka et al. 2004; Popesso et al. 2007). However, explaining cluster galaxy evolution using E+A galaxies may no longer be realistic.

One explanation for E+A phenomena is dust-enshrouded star formation, where E+A galaxies are actually star-forming, but emission lines are invisible in optical wavelengths due to heavy obscuration by dust (e.g., Poggianti & Wu 2000). A straightforward test for this scenario is observation in radio wavelengths in which dust obscuration is negligible. At 20-cm radio wavelengths, synchrotron radiation from electrons accelerated by supernovae can be observed. Therefore, in the absence of a radio-loud active nucleus, the radio flux of a star-forming galaxy can be used to estimate its current massive star formation rate (SFR) (Condon 1992; Kennicutt 1998; Hopkins et al. 2003). Smail et al. (1999) observed $z=0.4$ cluster in radio, and found that 5 out of 10 radio sources show E+A like spectra in optical wavelength. Chang et al. (2001) observed 5 nearby field E+A galaxies and detected no radio continuum. Miller & Owen (2001) observed radio continua of 15 E+A galaxies and detected moderate levels of star formation in only 2 of them. Goto (2004) undertook 20-cm radio continuum observation of 36 E+A galaxies and none of them were detected at 20-cm, suggesting that E+A galaxies are not dusty-starburst galaxies.

It is well-known that a galaxy-galaxy interaction triggers off explosive star formation (e.g., Schweizer 1982; Lavery & Henry 1988; Liu & Kennicutt 1995a,b; Schweizer 1996; Nikolic, Cullen & Alexander 2004). Oegerle, Hill & Hoessel (1991) found a nearby E+A galaxy with a tidal tail feature. High-resolution Hubble Space Telescope imaging supports the galaxy-galaxy interaction scenario by showing some post-starburst (E+A) galaxies in high-redshift clusters as having disturbed or interacting signatures (Couch et al. 1994, 1998; Dressler et al. 1994; Oemler, Dressler & Butcher 1997). Norton et al. (2001) performed long-slit spectroscopic observations of 21 E+A galaxies, and found that young stellar populations of E+A galaxies are more centrally concentrated than older populations, and old components of E+A galaxies conform to the Faber-Jackson relation. Bartholomew, Rose & Gaba (2001) reported that E+A galaxies, on average, tend to have slightly bluer radial gradients toward the centre compared to normal early-type galaxies. Yang et al. (2004) presented HST observations of the five bluest E+A galaxies with $z < 0.1$ and reported details of disturbed morphologies. Moreover, Yang et al. (2004) detected compact sources associated with E+A galaxies consistent with the brightest clusters in nearby starburst galaxies. Yamauchi & Goto (2005) not only showed obvious bluer radial colour gradients but also found irregular structures in their two-dimensional (2-D) colour map. Yagi & Goto (2006) and Yagi, Goto & Hattori (2006) investigated the age distribution using long-slit spectroscopy and found a positive gradient in the age of young stars from the centre to the outer regions of the plume. Recently, some numerical simulations on E+A galaxies have also been presented. Bekki, Shioya & Couch (2001) modelled galaxy-galaxy mergers with dust extinction, confirming that such systems can produce spectra that evolve into E+A spectra. Bekki et al. (2005) in-

vestigated the structural, kinematical and spectrophotometric properties of E+A galaxies, and showed that the 2-D distributions of line-of-sight velocity, velocity dispersion, colour and line index in E+A galaxies formed via the interaction and merging of two gas-rich spirals.

Thus, many studies have been conducted on the large-scale environments and internal properties of E+A galaxies, and recent studies basically support the merger/interaction origin of E+A galaxies. Several studies have focused on the medium-scale environments of E+A galaxies, e.g., Blake et al. (2004), Goto (2003) and Goto (2005). Using SDSS imaging data, Goto (2003) found that young E+A galaxies have more accompanying galaxies within 100 kpc. Results in Goto (2003) and Goto (2005) provide strong support for the merger/interaction origin of E+A galaxies, and we are interested in the physical relation between E+A galaxies and their accompanying galaxies. However, their studies are based on the imaging data, and not all accompanying galaxies are spectroscopically observed in the SDSS. In addition, it is unknown which galaxy is a real companion of E+A galaxies in Goto (2003) and Goto (2005).

Our aim is to extract some clues from medium-scale environments, that is, the physical relations between E+A galaxies and their pair galaxies, to investigate their evolution. However, we must confirm whether accompanying galaxies in Goto (2003) and Goto (2005) are companions, using statistical analyses with spectroscopic data. We will begin our studies on the properties of E+A galaxies and pair systems after such verification.

In this paper, we use publicly available *true* E+A galaxies (without H nor [O II] emission) selected from the Sloan Digital Sky Survey (SDSS, York et al. 2000; Early Data Release, Stoughton et al. 2002; First Data Release, Abazajian et al. 2003; Second Data Release, Abazajian et al. 2004; Third Data Release, Abazajian et al. 2005; Fourth Data Release, Adelman-McCarthy et al. 2006; Fifth Data Release, Adelman-McCarthy et al. 2007, hereafter DR5) by Goto (2007b). Both broadband imaging and the spectroscopic survey of 10,000 deg^2 of SDSS provide us with the first opportunity to study a very large number of E+A galaxies. Goto (2007b) analysed 670,000 galaxy spectra in the DR5, and the number of homogeneous E+A galaxies reached 1,062. We created the catalogue of companions/candidates of E+A galaxies using the SDSS SQL service, and we observed the spectra of companion candidates to reveal their redshifts. We then investigated an existing probability of companions of E+A galaxies by a stricter analysis with spectroscopic data.

This paper is organised as follows. In section 2, the definitions of two samples of galaxies are summarised. In section 3, we briefly describe our spectroscopic observations on companion candidates of E+A galaxies, and reduction of their data. In section 4, we explain a somewhat complicated method of statistical analysis for readers to more easily understand. In section 5, we show the application of the method described in section 4 to both the E+A sample and control sample, and present the results. Lastly, we provide a discussion and summary in section 6.

Unless otherwise stated, we adopt the best-fitting *Wilkinson Microwave Anisotropy Probe* (WMAP) cosmology: $(\Omega_b; \Omega_m; \Omega_\Lambda) = (0.071; 0.27; 0.73)$ (Bennet et al. 2003; Komatsu et al. 2008).

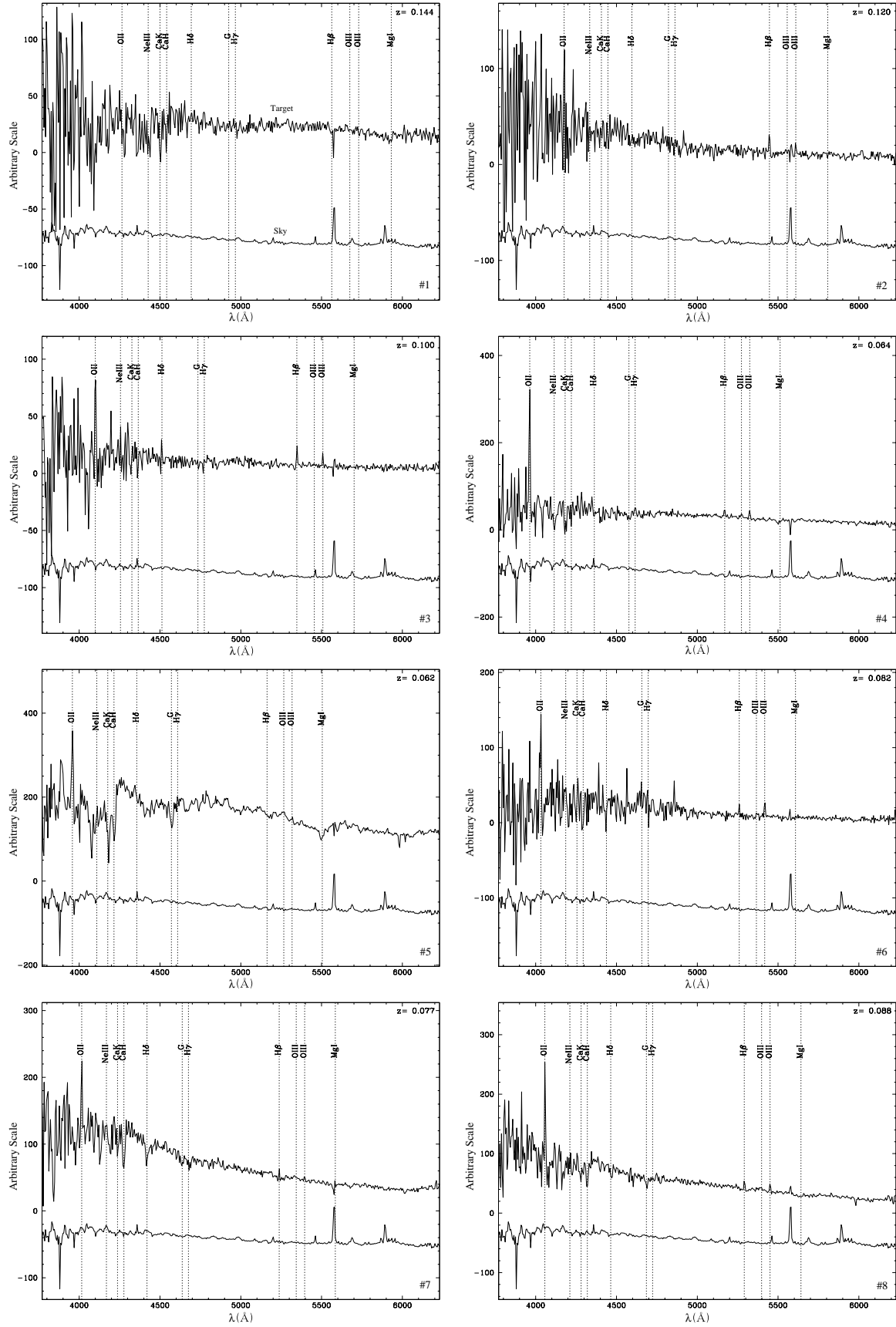


Figure 1. Spectra of 16 new E+A's companions taken with the KPNO 2.1-m telescope applying a 20\AA binning. A sky spectrum in the observed data is shown at the bottom of each panel. This figure includes targets #1(top left), #2(top right), ..., #7(bottom left) and #8(bottom right).

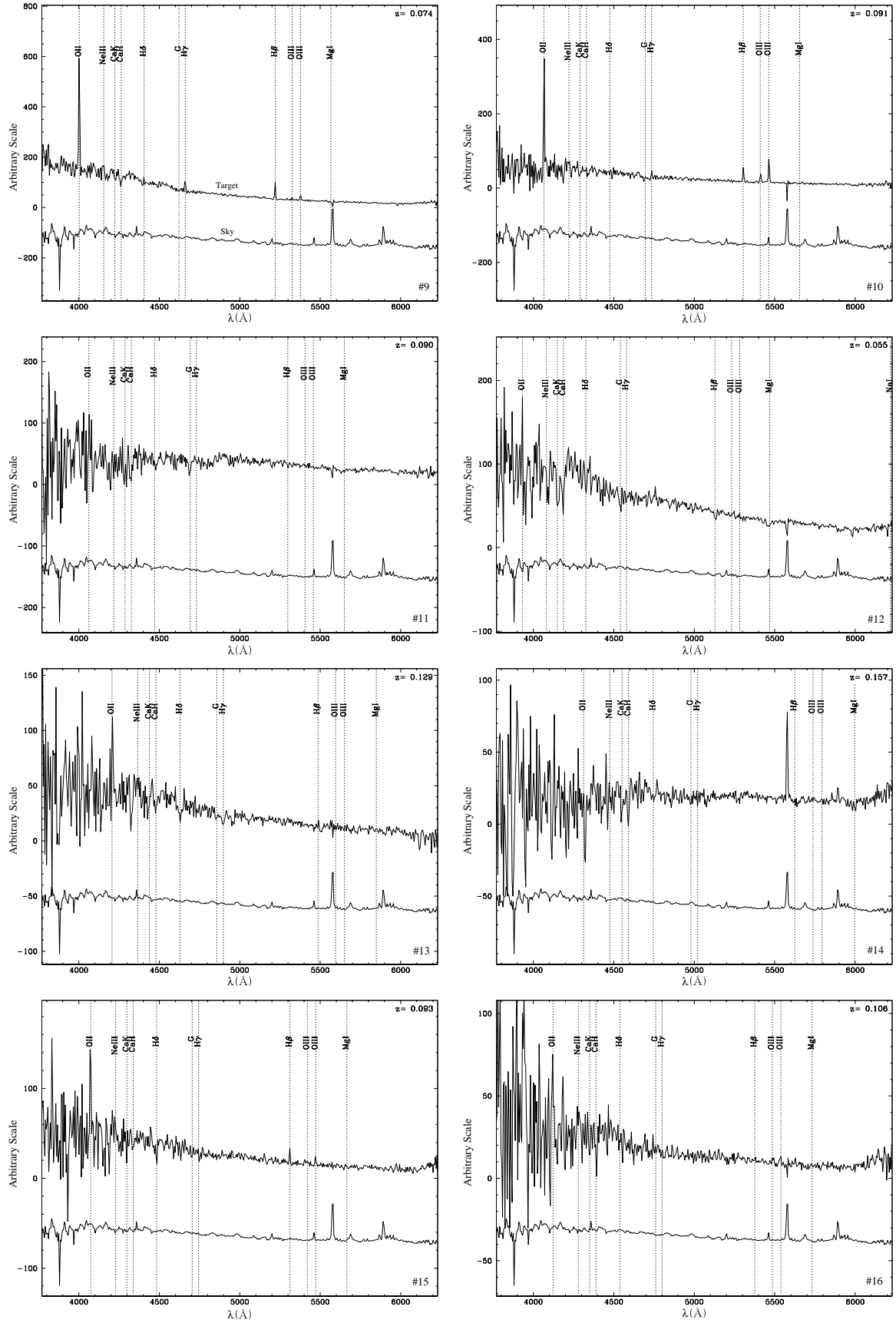


Figure 1 – continued targets #9(top left), #10(top right), ..., #15(bottom left) and #16(bottom right).

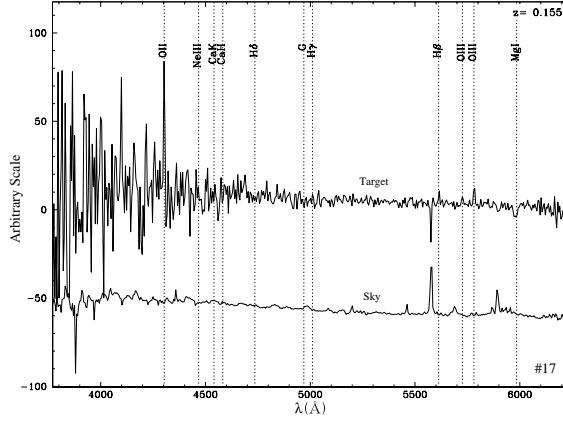


Figure 1 – continued target #17.

Table 1. List of E+A and companion pairs. Columns r and M_r are magnitudes and absolute magnitudes with reddening- and K -correction by `kcorrect.v4.1.4` (Blanton et al. 2003). Column elements of the “origin of z ” filled by italicised letters show information obtained by the NED search service. ID 25 or ID 26 is an “E+A and E+A” pair.

Pair ID	E+A galaxies							Companion galaxies							projection	
	R.A.	Dec.	r	M _r	z	H	E-W	R.A.	Dec.	r	M _r	z	origin of z	j	z _j	distance(kpc)
1	01:19:42.23	+01:07:51.5	16.75	-21.29	0.090	6.40		01:19:41.58	+01:07:39.9	17.63	-20.41	0.089	SDSS	0.001		25.18
2	07:53:23.09	+24:33:00.5	15.80	-21.36	0.061	5.74		07:53:22.80	+24:33:02.5	15.78	-21.38	0.062	SDSS	0.001		5.21
3	08:41:41.13	+26:42:39.2	16.97	-21.07	0.090	4.97		08:41:40.75	+26:42:41.2	17.23	-20.81	0.090	KPNO Observation #11	0.000		9.11
4	09:03:32.77	+01:12:36.4	16.16	-20.89	0.058	4.43		09:03:32.99	+01:12:31.7	17.39	-19.66	0.058	SDSS	0.000		6.32
5	09:25:03.81	+40:46:02.8	17.69	-20.97	0.117	4.90		09:25:04.65	+40:45:55.3	16.53	-22.12	0.117	SDSS	0.000		25.25
6	09:58:24.62	+00:32:03.1	17.15	-20.96	0.093	5.50		09:58:24.08	+00:32:06.4	17.45	-20.66	0.093	KPNO Observation #15	0.000		14.89
7	10:05:22.45	+07:27:28.3	16.95	-20.28	0.063	4.92		10:05:21.12	+07:27:25.9	15.38	-21.85	0.064	KPNO Observation #4	0.001		23.99
8	10:16:29.22	-00:01:37.1	17.37	-21.02	0.105	5.90		10:16:28.55	-00:01:34.3	17.86	-20.54	0.105	<i>MGC 0004420</i>	0.000		19.43
9	10:57:49.08	+41:00:35.9	17.50	-21.38	0.128	4.05		10:57:47.54	+41:00:49.2	17.16	-21.72	0.128	SDSS	0.000		49.89
10	11:10:04.24	+11:51:19.7	15.45	-22.25	0.078	4.13		11:10:03.74	+11:51:23.1	17.10	-20.61	0.077	KPNO Observation #7	0.001		11.78
11	11:41:38.76	+09:43:44.6	17.64	-20.07	0.078	4.64		11:41:36.84	+09:43:35.6	15.46	-22.25	0.079	SDSS	0.001		43.52
12	11:52:08.57	+48:16:58.4	17.24	-19.67	0.055	5.88		11:52:07.36	+48:17:22.7	16.66	-20.25	0.055	KPNO Observation #12	0.000		28.52
13	11:56:28.91	+48:55:41.6	17.72	-19.99	0.078	4.06		11:56:27.66	+48:55:39.9	16.51	-21.20	0.078	SDSS	0.000		18.14
14	12:13:33.02	+14:29:00.1	16.26	-21.01	0.064	5.94		12:13:34.12	+14:28:42.4	15.94	-21.33	0.064	SDSS	0.000		28.90
15	12:22:40.46	+15:02:05.4	17.72	-19.82	0.072	8.10		12:22:40.76	+15:02:22.3	15.67	-21.88	0.072	SDSS	0.000		23.73
16	13:00:29.45	+54:55:04.0	16.60	-21.41	0.089	4.81		13:00:32.15	+54:54:57.9	16.65	-21.36	0.088	KPNO Observation #8	0.001		39.44
17	13:30:24.73	+02:23:25.8	17.33	-20.41	0.079	5.66		13:30:23.85	+02:23:04.3	15.67	-22.06	0.079	SDSS	0.000		37.22
18	13:50:05.58	-02:47:34.7	16.71	-22.16	0.128	5.81		13:50:05.89	-02:47:38.8	17.94	-20.93	0.129	KPNO Observation #13	0.001		14.02
19	13:50:50.98	+02:19:38.4	15.85	-19.90	0.033	4.59		13:50:53.55	+02:19:24.6	14.28	-21.46	0.033	<i>UGC 08750 NED01</i>	0.000		26.25
20	14:24:53.14	+23:07:46.8	15.70	-21.89	0.074	4.05		14:24:52.86	+23:07:20.9	16.82	-20.77	0.074	KPNO Observation #9	0.000		36.24
21	14:36:33.54	+55:53:17.8	17.60	-20.78	0.104	4.08		14:36:31.82	+55:53:27.6	16.65	-21.74	0.105	SDSS	0.001		32.96
22	14:50:33.38	+03:18:20.0	17.33	-19.86	0.062	4.04		14:50:31.09	+03:18:03.5	16.89	-20.30	0.062	SDSS	0.000		44.90
23	15:13:09.04	+33:49:44.4	17.47	-21.84	0.155	5.05		15:13:07.74	+33:49:51.4	19.48	-19.83	0.155	KPNO Observation #17	0.000		46.63
24	15:34:16.00	+03:59:34.6	17.71	-21.65	0.157	4.55		15:34:16.19	+03:59:33.4	18.32	-21.03	0.157	KPNO Observation #14	0.000		8.27
25	15:57:28.87	+27:25:45.2	16.43	-21.55	0.087	4.22		15:57:30.42	+27:25:41.1	17.30	-20.68	0.088	SDSS	0.001		34.10
26	15:57:30.42	+27:25:41.1	17.30	-20.69	0.088	4.11		15:57:28.87	+27:25:45.2	16.43	-21.56	0.087	SDSS	0.001		34.23
27	16:13:30.18	+51:03:35.5	15.48	-20.34	0.034	7.57		16:13:32.23	+51:03:42.9	15.17	-20.65	0.033	<i>IZw 136 NOTES02</i>	0.001		13.64
28	16:21:51.96	+49:28:59.8	17.04	-20.79	0.082	4.26		16:21:55.07	+49:29:08.0	18.21	-19.62	0.082	KPNO Observation #6	0.000		47.84
29	16:23:01.30	+23:00:39.8	17.48	-19.69	0.061	4.73		16:23:01.04	+23:01:12.0	14.89	-22.28	0.062	KPNO Observation #5	0.001		37.84
30	16:23:17.62	+32:45:26.8	17.73	-20.32	0.090	4.65		16:23:17.42	+32:45:02.3	17.24	-20.81	0.091	KPNO Observation #10	0.001		40.97
31	16:39:25.01	+30:37:09.8	17.56	-20.86	0.106	8.23		16:39:24.87	+30:37:15.3	18.00	-20.42	0.106	KPNO Observation #16	0.000		11.09
32	16:56:48.64	+31:47:02.3	16.70	-21.58	0.100	5.75		16:56:48.32	+31:47:02.3	18.63	-19.66	0.100	KPNO Observation #3	0.000		13.39
33	17:03:56.71	+62:28:48.3	17.64	-21.53	0.145	7.29		17:03:55.12	+62:28:56.0	18.03	-21.14	0.144	KPNO Observation #1	0.001		33.89
34	17:08:59.24	+32:20:53.1	17.58	-21.14	0.121	6.03		17:08:59.03	+32:21:00.3	18.08	-20.65	0.120	KPNO Observation #2	0.001		16.49

2 SAMPLES

Our statistical analysis requires E+A and control samples and their companions/candidates, and the redshifts of some candidates are measured by our observations. We describe our method for creating these samples in this section.

Galaxies used in our study are taken from the SDSS DR5 (Adelman-McCarthy et al. 2007). Details of the photometric system, imaging hardware and astrometric calibration of the SDSS are described in Fukugita et al. (1996); Gunn et al. (1998); Hogg et al. (2001); Smith et al. (2002); Strauss et al. (2002); Pier et al. (2003). Our E+A galaxies are selected from a publicly available catalogue described in Goto (2007b). We created a catalogue of companions/candidates of E+A galaxies and a comparison sample of normal galaxies. These samples satisfy an absolute magnitude of $-22.5 < M_r < -19.5$ (k- and Galactic extinction corrected) using the SDSS Catalogue Archive Server (CAS). This absolute magnitude range is adopted so that the control sample of normal galaxies should be volume-limited.

2.1 Parent Galaxies

The SDSS DR5 catalogue contains 670,000 galaxies with spectroscopic information. Goto (2007b) selected 1062 E+A galaxies which satisfy $4.0\text{\AA} < H_{EW}$, $3.0\text{\AA} < H_{EW}$ and $2.5\text{\AA} < [OII]_{EW}$ (absorption lines have a positive sign). The E+A galaxies are selected in an unbiased way except for the redshift cut ($z > 0.032$) and the S/N cut (> 10 per pixel in r-band wavelength). The redshift cut guarantees a reliable measurement of $[OII]_{EW}$ since the blue limit of the SDSS spectrum is 3800\AA . The spectroscopic data, H_{EW} , H_{EW} and $[OII]_{EW}$ equivalent width (EW) and their errors are measured by the flux-summing method described in Goto (2007b) (See also Goto 2003).

Our targets have an absolute magnitude of $-22.5 < M_r < -19.5$ and $z < 0.167$. These criteria assure all targets are brighter than $r = 20.0$, and thus, can be observed spectroscopically with the KPNO 2.1-m telescope. This selection leaves 660 E+A *parent*² galaxies around which we spectroscopically look for companion galaxies. We use these as our sample for statistical study.

A control sample is selected from all objects classified as galaxies in the SDSS DR5 catalogue. The magnitude range of the SDSS spectroscopy that satisfies high completeness and reliability is $14.5 < r < 17.7$. We obtain r-band distance modulus $(m - M)_r = 37$ at $z = 0.06$. Therefore, we can set the limit of redshift (z) between 0.0570 and 0.0620 so that the sample satisfies the volume-limited condition with $-22.5 < M_r < -19.5$; then we obtain 11,267 *parent* normal galaxies as a control sample.

The control sample and the E+A sample are selected from the different redshift ranges ($0.032 < z < 0.167$ and $0.0570 < z < 0.0620$, respectively). However, both of the redshift ranges are small and close to $z = 0$, and thus, we assume that evolutionary differences such as change of merger rate between two samples are small enough in our samples.

2.2 Companion/Candidate Galaxies

To investigate the number of parent galaxies that have companion galaxies, we created a catalogue of companion candidates for our

E+A sample and control sample using a photometric catalogue. The companion candidates are selected within the region of 50-kpc radius centred on the parent galaxy in the sky. The candidate catalogue is constructed by executing the `fGetNearbyObjEq()` function built in the SDSS SQL service for each parent galaxy. We calculated the absolute magnitude M_r of candidates assuming that they are placed at the redshift of the parent galaxy, and then removed candidates whose M_r do not satisfy $-22.5 < M_r < -19.5$. The numbers of parent E+A and normal galaxies that have companions or candidates are 97/660 and 791/11267, respectively.

The next step is to distinguish the true companion galaxies from the candidates. We obtained the redshifts of the candidate galaxies that have `SpecObjID` from the SDSS SQL server, and selected the true companions. In addition to this, we utilized the redshift information in the NED database whenever available. We used the criterion of $z_j - 0.002$ to decide whether a candidate galaxy is a true companion. The escape velocity of a $M_r = -22.5$ galaxy is 200km/s , when $M_r = L_r / 3$ (Kauffmann et al. 2003) is assumed. Therefore, the criteria of $z_j = 0.002$, that is, $v < 600\text{km/s}$, is large enough not to miss any gravitationally bound galaxies. We use the notation ‘companions’ for the galaxies that satisfy the criteria throughout this paper.

3 OBSERVATION WITH THE KPNO 2.1-M TELESCOPE

There are many companion candidates without spectroscopic redshift of E+A galaxies in our catalogue created in section 2.2. We used the KPNO 2.1-m telescope to obtain some of their spectroscopic redshifts.

We used the GoldCam spectrometer attached to the 2.1-m telescope at the KPNO. The aim of this observation was to identify the true companions of E+A galaxies. This purpose can be achieved by obtaining spectra of accompanying galaxies from the SDSS photometric catalogue since we already know the redshifts of parent E+A galaxies. We used the 26new grating with the long-slit of 2300 arcsec. The CCD for the spectroscopy is $3,072 \times 1,024$ pixel whose resolution is 0.78 arcsec/pixel and 5\AA . We used a quartz lamp and HeNeAr calibration source built in the GoldCam for flat and comparison, respectively.

The targets were selected from companion candidates without spectroscopic redshifts. Our observation was carried out in three semesters. We observed 26 companion candidates³ on September 22-24, 2005, June 28, 2006 and May 17-21, 2007. The data reduction were performed with the NOAO/IRAF V2.12.2. The `ccdproc` task in `noao/imred/ccred` package was used for the overscan reduction and zero, dark and flat corrections. The comparison, zero, dark and target frames were simply combined by the `imcombine`, but the flat frames were combined after being divided by the mean value calculated by the `imstat` task.

The wavelength calibration was performed by `identify`, `reidentify` and `fitcoords` tasks using a HeNeAr comparison data. The `transform` task transforms long-slit images to wavelength co-ordinates using the calibration database. After carefully subtracting the background by the `background` task, we traced the signal of the target frame with a 4-pixel aperture by the `apall` task.

Our companion candidates included some passive galaxies

² Note that the magnitude or physical size of the ‘parent galaxy’ is not always larger than that of ‘companion galaxies’ in this paper.

³ Actually we observed 28 candidates in total, including two backup targets. See APPENDIX 1.

and galaxies fainter than $r = 19$ magnitude. The S/N of such objects cannot be poor (S/N > 1) when using the 2.1-m telescope: therefore, sometimes it was difficult to identify their redshifts.

In summary, we identified the redshifts of 19 targets and could not identify those of 7 targets. We found that these galaxies with spectroscopic redshift included 17 true companions. We show their spectra in Figure 1. Table 1 also includes basic data of these successful targets.

4 BASIC METHOD OF STATISTICAL ANALYSIS

The goal of our study is to compare the fractions of galaxies that have companions within a defined region (e.g., within a 50-kpc radius) in the sky, for E+A and control samples. If the redshift of all galaxies are already known, we can easily count the number of parent galaxies with companions. However, many galaxies have no spectroscopic data, and we cannot know whether the galaxy is a companion or a chance overlap. Therefore, we have to estimate the fraction of galaxies having companions using statistical analysis. We describe the analytical method in this section.

4.1 Estimation of the number of companion galaxies within a defined region

The companion candidates in the constructed catalogue can be divided into following groups:

g_t : companions with spectroscopic redshifts,
 g_f : fore/background galaxies with spectroscopic redshifts,
 g_u : companion candidates without spectroscopic redshifts.
 We define n_t , n_f and n_u as the number of g_t , g_f and g_u galaxies, respectively. The following notations are also defined:
 n_{os} : number of accompanying galaxies with spectroscopic data
 n_{op} : number of accompanying galaxies with photometric data
 That is, $n_{os} = n_t + n_f$ and $n_{op} = n_t + n_f + n_u$. The actual flow is presented in the top panel in Figure 2; the problem is the number of true companions in g_u .

The number of *all* companion galaxies, n_{et} , is the sum of the number of true companions (n_t) and the number statistically estimated, which is a part of n_u . We assume that the target selection of SDSS spectroscopy is unbiased (Strauss et al. 2002). Under the assumption, the existing probability of companions in the photometric sample equals the probability in the spectroscopic sample. We can derive

$$\frac{n_{et}}{n_{op}} = \frac{n_t}{n_{os}}; \quad (1)$$

The expected number of companions per a parent galaxy within a defined region, i , is therefore obtained by

$$i = \frac{n_{et}}{N_M}; \quad (2)$$

where N_M is the number of parent galaxies. In this study, we use lowercase g and n for group and number of companion/candidate galaxies, and uppercase G and N for those of parent galaxies.

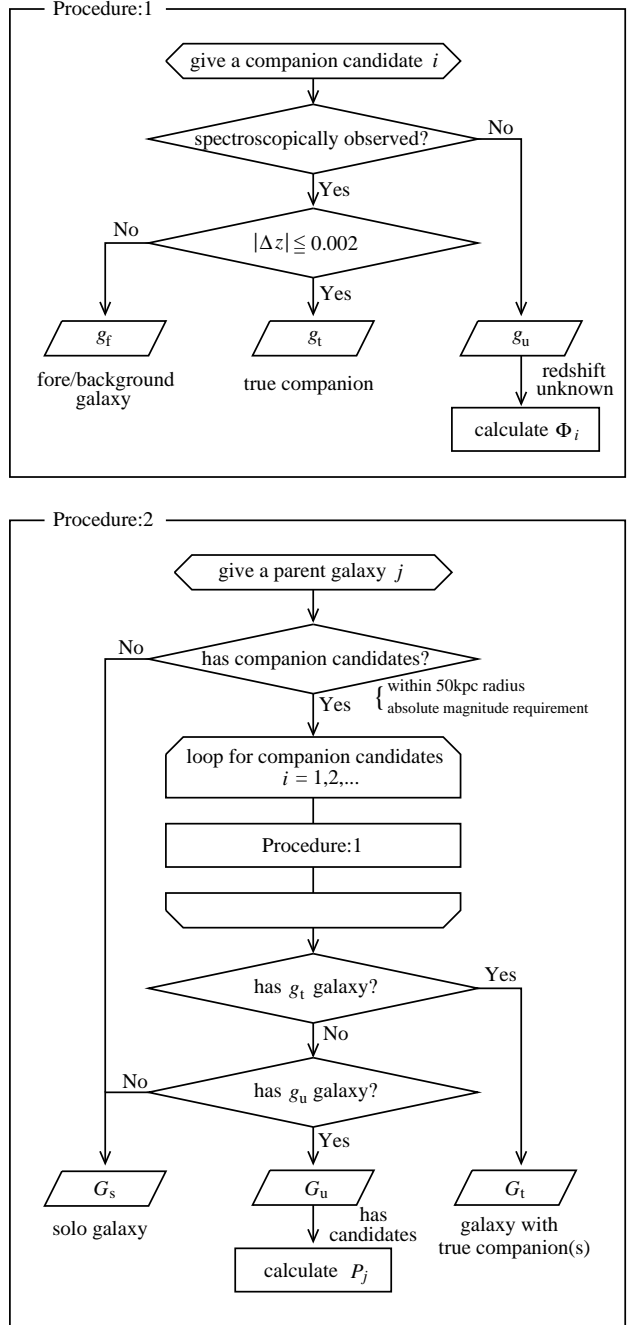


Figure 2. Basic flow of our analysis. Top panel ‘procedure:1’ shows the flow about a given companion candidate, and the bottom panel ‘procedure:2’ shows that about a given parent galaxy. ‘Procedure:1’ is used in ‘procedure:2’.

4.2 Estimation of number of parent galaxies that have companions

The parent galaxies are also divided into three groups:

G_t : galaxies that have true companions (may also have candidates without redshift or fore/background galaxies),

G_s : solo galaxies (around which there may be fore/background galaxies with spectroscopic redshifts),

G_u : galaxies that have no true companions but have candidates without spectroscopy (around which there may also be fore/background galaxies with spectroscopic redshifts)

The targets for spectroscopic observation at the KPNO are selected from the G_u group. Note that we selected the parent galaxies from the spectroscopic catalogue, and we therefore know the redshifts of the parent galaxies. We show the overview of this grouping procedure in the bottom panel in Figure 2. Our goal is to obtain the number of G_t plus the number of a portion of G_u , since a companion candidate without spectroscopy is either ‘a true companion’ or ‘a back/foreground galaxy’. The problem is the estimation of the probability of existing companions in G_u galaxies.

A companion candidate without spectroscopy is either ‘a true companion’ or ‘a back/foreground galaxy’. The probability that a candidate i is a true companion, p_i , can be calculated by

$$p_i = \frac{\bar{n}_i}{\bar{n}_t}; \quad (3)$$

where \bar{n}_i is the expected number of galaxies within the corresponding field of view (FOV) of a certain physical area in which the parent galaxy is centrally placed.

Allocating the probability p_i to each companion candidate i of the parent galaxies in G_u , we can calculate the probability that the parent galaxy j has at least one true companion by

$$P_j = 1 - \prod_i (1 - p_i); \quad (4)$$

In group G_u , the expected number of galaxies that have companion galaxies, N_e , is the summation of P_j of each parent galaxy j ,

$$N_e = \sum_j P_j; \quad (5)$$

We can thus estimate the number of parent galaxies with companion galaxies as

$$N_{et} = N_t + N_e; \quad (6)$$

where N_t is the number of galaxies in G_t .

5 ANALYSIS AND RESULTS

Using the method described in section 4, we estimated the number of companion galaxies of control sample and E+A sample. As described in section 2, the control sample is made from SDSS DR5 with $0.0570 < z < 0.0625$ and $22.5 < M_r < 19.5$. The E+A sample is made from Goto (2007b) with $z < 0.167$ and $22.5 < M_r < 19.5$. The companions/candidates are selected in the aperture of a 50-kpc radius in which each parent galaxy is centrally placed, so that they satisfy $22.5 < M_r < 19.5$. The redshift criterion of control sample guarantees that the sample is volume-limited both for the parents and the companions. We analysed these galaxies as follows.

Table 2. Number counts of galaxies ≤ 50 (per 0.5 mag deg⁻²) in the r-band within the corresponding FOVs of 50-kpc radius for 5 redshift regions. N_p is the number of parent galaxies centrally placed in the FOVs, and n_f is the number of found galaxies in the FOVs in total.

Mag Range (r)	z:0.03-0.06	z:0.06-0.09	z:0.09-0.12	z:0.12-0.15	z:0.15-0.18
13.0-13.5	0.550	0.408	0.0	0.0	0.0
13.5-14.0	2.31	0.316	0.688	2.42	0.0
14.0-14.5	5.00	0.836	0.539	0.0	0.0
14.5-15.0	9.91	4.21	0.947	0.939	0.0
15.0-15.5	14.7	13.9	6.279	6.230	2.03
15.5-16.0	17.9	23.6	21.2	5.345	6.53
16.0-16.5	30.3	34.8	42.7	28.6	17.4
16.5-17.0	36.1	47.3	75.8	68.9	54.0
17.0-17.5	49.6	70.8	87.0	111.4	114.2
17.5-18.0	83.2	103.8	158.2	189.7	265.8
18.0-18.5	151.2	176.3	230.6	366.8	430.2
18.5-19.0	227.5	263.0	359.1	480.3	645.8
19.0-19.5	378.1	389.3	528.5	626.1	864.3
19.5-20.0	605.8	676.1	752.3	975.1	1211
20.0-20.5	944.7	1010	1242	1419	1714
20.5-21.0	1415	1493	1698	1966	2399
21.0-21.5	2032	2181	2395	2734	3146
N_p	5807	12481	10061	8538	5782
n_f	27267	25447	12915	8382	4949

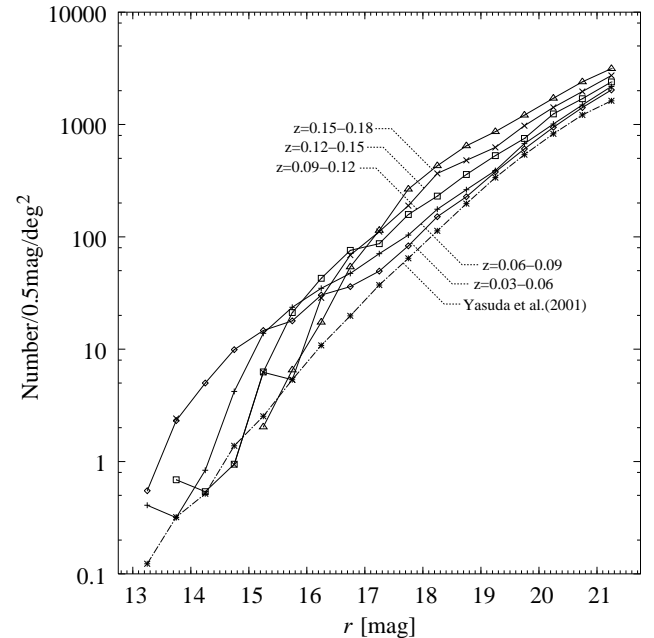


Figure 3. Plot of number count in Table 2 and the result of Yasuda et al. (2001). Our number count of 5 redshift regions are drawn by solid line, and the dot-dashed line is the count of Yasuda et al. (2001).

5.1 Number counts within FOVs of a 50-kpc radius

For calculating probability in equation (3), number counts of fore/background galaxies are required. Yasuda et al. (2001) provides the number counts of galaxies using SDSS data. The result shown in Yasuda et al. (2001) is the average of all observed region. However, galaxies are not randomly distributed but tend to cluster.

Table 3. Number count of true companions n_t , estimated number of all companions n_{et} and expected number of companions per a parent galaxy $\langle M_r \rangle$, for the control sample within each defined magnitude.

	n_t	n_{et}	
20:56 $M_r < 19:5$	109	276	0.0245
21:56 $M_r < 20:5$	93	235	0.0209
22:56 $M_r < 21:5$	41	104	0.00921
all	243	615	0.0546

Therefore, we can expect that the number count around a galaxy would be higher than that of random field by Yasuda et al. (2001).

The required data for our analysis are the number counts of the field of view within a 50-kpc radius in which each parent galaxy is centrally placed. The corresponding apparent size of 50-kpc radius is changed according to the redshift of the parent galaxy. Therefore, we construct the data of number counts of galaxies per area for 5 redshift ranges, 0.03-0.06, 0.06-0.09, 0.09-0.12, 0.12-0.15 and 0.15-0.18.

The r -band number count in 50-kpc circular region of each redshift range, $n_{50}(z;r)$, is calculated by

$$n_{50} = \frac{1}{N_p} \sum_j \sum_i \frac{n_{fj}}{A_{fov_j}} A_{fov_i}; \quad (7)$$

where N_p is the number of parent galaxies ($22:5 < M_r < 19:5$) in the corresponding redshift range, n_{fj} is the number of found galaxies in the apparent magnitude range in the FOV of 50-kpc radius around the parent galaxy j , and A_{fov_j} is the area of FOV. We randomly selected 42,669 parent galaxies within $0:03 < z < 0:18$ and $22:5 < M_r < 19:5$ from all galaxies in SDSS DR5. The galaxies within a 50-kpc radius was selected by executing the `fGetNearbyObjEq()` function built in the SDSS SQL service for each parent galaxy.

In total 78,960 galaxies of $13:0 < r < 21:5$ were selected by `fGetNearbyObjEq()`. The result of n_{50} for each redshift range is shown in Table 2 and Figure 3. This figure shows that we cannot ignore the effects of galaxy correlation in our study. In section 5.2 and 5.3, we use $n_{50}(z;r)$ values in Table 2 for the number counts in the FOVs when applying⁴ equation (3).

5.2 Control sample

After constructing the catalogue of companion candidates which belongs 11,267 normal galaxies⁵ within $0:05706 < z < 0:0620$, we divided the candidates into three groups according to the absolute magnitude of the r -band, M_r . That is, we set the two thresholds of M_r , 20:5 and 21:5, for candidates.

Even if the magnitude range of a sample obtained from the SDSS photometric catalogue satisfies the limit of SDSS spectroscopy ($14:5 < r < 17:7$), the sample is not complete for the spectroscopic data, for example because of fibre collision. Therefore, we counted n_{os} (accompanying galaxies with spectroscopic data) and n_{op} (accompanying galaxies with photometric data), and

Table 4. Summary of the numbers in this study. N_M is the number of parent galaxies, and N_{et} is the estimated number of parent galaxies with true companions. See the text for other notations.

	N_M	n_{op}	n_{os}	n_t	N_t	N_u	N_e	N_{et}
Control sample	11267	1035	409	243	241	550	336	577
E+A sample	660	119	41	34	34	63	18.0	52.0

obtained $n_{os} = 409$ and $n_{op} = 1035$. In Table 3, we showed n_t (number of the true companions), n_{et} (the estimated number of all companion galaxies from equation (1)), and $\langle M_r \rangle$ (the expected number of companions per a parent galaxy from equation (2)) of three absolute magnitude ranges.

We can then calculate the number of parent galaxies for each group. In this control sample, the number of G_t (galaxies that have true companions), N_t , is 241, and that of G_u (galaxies that have no true companions but have candidates without spectroscopy), N_u , is 550. The P_j in equation (5) is calculated by equation (4). And p_i , the probability that a candidate is a true companion, is calculated by equation (3). In equation (3), n_{50} and A_{fov_i} are required for each companion candidates. n_{50} is obtained from Table 3, and A_{fov_i} is derived as

$$A_{fov_i} = n_{50}(z;r) \cdot A_{fov_j}; \quad (8)$$

where A_{fov_j} is the area corresponding to the region of a 50-kpc radius and $n_{50}(z;r)$ is the number count of galaxies in Table 2. We use absolute magnitude of the candidate for n_{50} , and use apparent magnitude of the candidate for A_{fov_j} .

We obtained $N_e = 336$ and $N_{et} = 577$. This indicates that 5.12% ($= 577/11267$) of normal galaxies have companion galaxies within a 50-kpc radius. The numbers are shown in Table 4.

5.3 E+A sample

Following the description in section 2, we constructed the companion candidate catalogue for E+A galaxies. We found $n_{op} = 119$ of photometrically observed companion candidates, and 19 of the candidates were spectroscopically observed in the SDSS. Our KPNO observations appended 19 redshifts of companion candidates, and we found 3 redshifts of candidates from the NED search service. The number of spectroscopically observed candidates then became $n_{os} = 41$. We found 14 true companions from SDSS and 17 true companions from our KPNO observation, and we found 3 true companions from the NED search service. That is, 7 objects turned out to be fore/background galaxies. Therefore, the number of true companion galaxies n_t is 34 in the G_{os} . As a result, $N_t = 34$ of E+A galaxies have true companions and $N_u = 63$ of E+As have candidates with no spectroscopy. We present the 34 E+A and companion systems in Table 1 and Figure 4.

We then estimate the number of E+As with companions (N_{et}) in the 63 galaxies. Since the redshift range of E+A sample is large, the E+A sample does not satisfy the volume-limited condition, and we cannot estimate the expected numbers of companions $\langle M_r \rangle$. Therefore we used the $\langle M_r \rangle$ of the control sample (Table 3) for the estimation of number of G_u E+A galaxies, following the null hypothesis that the probability of existence of companion is the same for E+A and normal galaxies. However, if the fraction of parent galaxies with companions in the E+A sample is really larger than that in the control sample, $N_{et} = N_M$ of the E+A sample and that of the control sample will show a significant difference even

⁴ We did not use any interpolations when applying values of Table 2, since the interpolations did not affect our statistical results.

⁵ These galaxies include 15 E+As. However, excluding these E+As does not affect our statistical results.

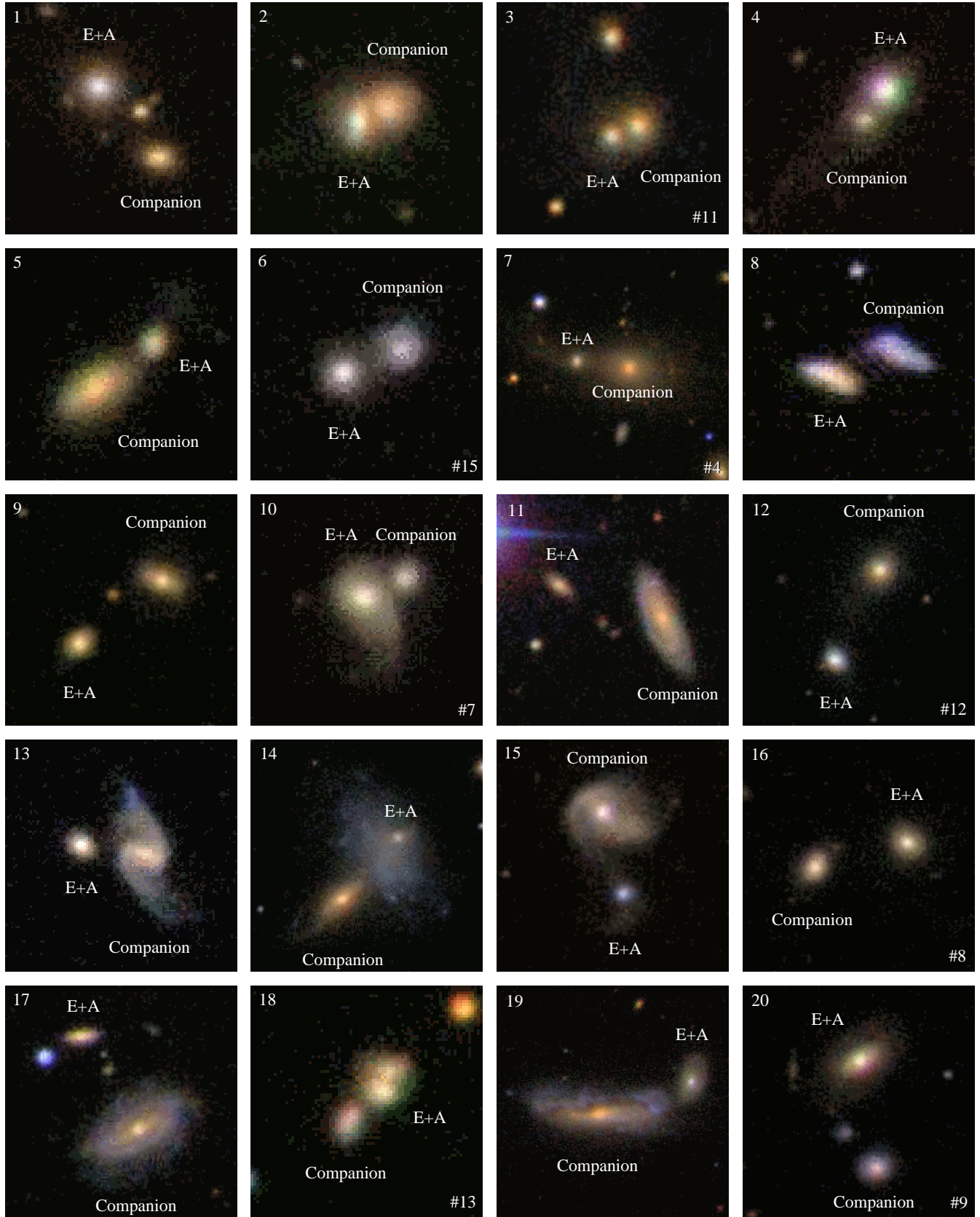


Figure 4. SDSS g,r,i -composite images of E+A and companion pairs taken from SDSS CAS. This figure includes pair ID no.1(*top left*), ... , no.4(*top right*), ..., no.17(*bottom left*), ... and no.20(*bottom right*). The inlaid number at the bottom right in each image is the target ID of our KPNO observation.

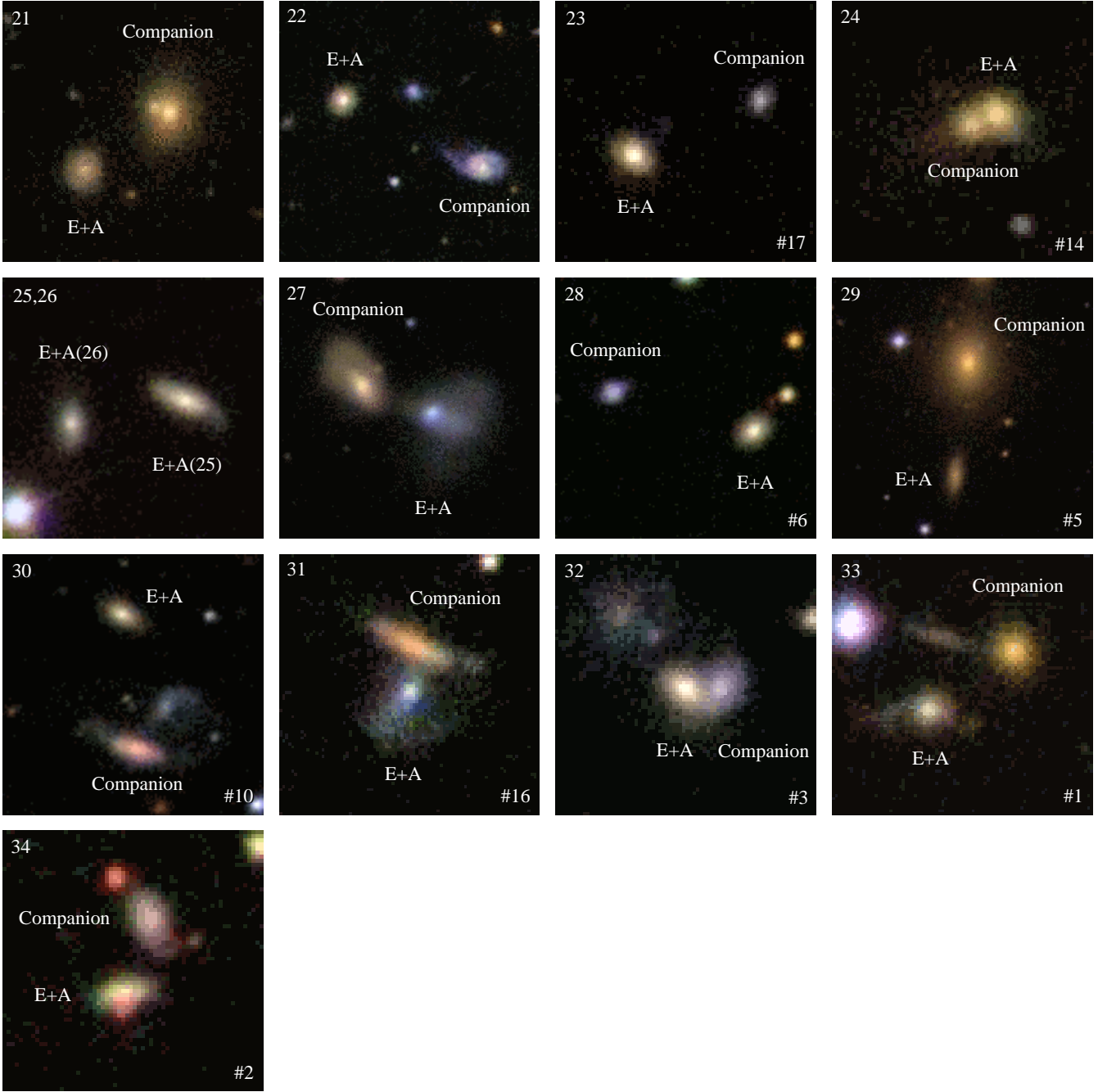


Figure 4 – *continued* Pair ID No.21(*top left*), ... , No.24(*top right*), ... and No.34(*bottom left*).

adopting the hypothesis. As described in section 5.2, we estimate the number of E+As with companions (N_{et}). Equation (4) – (6) resulted that the estimated N_{e} and N_{et} of E+A sample were 18.0 and 52.0, respectively. These results are summarised in Table 4.

The result indicates that at least 7.88% ($= 52.0/660$) of E+A galaxies have companion galaxies. In section 5.2, we found 5.12% ($= 577/11267$) of normal galaxies have at least one companion, i.e., E+A galaxies have 54% higher probability to do that. How statistically significant is this result? We applied a two-sample test for equality of proportions with continuity correction to answer the question. We used the `prop.test()` function of R

(<http://www.r-project.org/>) version 2.0.1. We set the parameter as `prop.test(c(52.0, 577), c(660, 11267))`, whereupon we achieved a 99.7% level of significance that the existing probabilities of companion galaxies are statistically different between the E+A (7.88%) and control samples (5.12%).

Although it was pointed out previously that E+A galaxies might have more companion galaxies than normal galaxies, this work is the first to show the result based on spectroscopic data, with statistical meaningful significance.

6 DISCUSSION AND SUMMARY

We constructed the first catalogue of E+A with companion galaxies based on spectroscopic data. The catalogue provides a basis for discussing the statistical analysis of E+A and companion systems. In section 5, we statistically showed that E+A galaxies have by 54% more companion galaxies than the control sample of normal (average) galaxies within 50 kpc. This result is a major step forward on the subject in that the analysis is based on the spectroscopic redshift survey of companion candidates; Although previous studies have suggested that E+A galaxies have more companions, some were based on mere a morphological impression of E+A galaxies (Oegerle, Hill & Hoessel 1991; Couch et al. 1994, 1998; Dressler et al. 1994; Oemler, Dressler & Butcher 1997; Yang et al. 2004; Yamauchi & Goto 2005), while others relied on the statistical analysis of imaging data (Goto 2005), which suffered from a large uncertainty from foreground/background galaxies. Our findings are much more reliable in that the analysis is based on spectroscopic data; that is, the 34 companion galaxies found in this work truly are in physically close proximity where they can dynamically interact with the central E+A galaxy. Therefore, our finding greatly strengthens the physical interpretation of the result; physical interaction/merger with companion galaxies is likely the origin of E+A galaxies.

Previous observational studies, for example, morphologies, radial photometric/spectroscopic analysis (Bartholomew, Rose & Gaba 2001; Yang et al. 2004; Yamauchi & Goto 2005) and numerical simulations (Bekki, Shioya & Couch 2001; Bekki et al. 2005) become much more realistic with our redshift identifications of companion galaxies. Taken together, little doubt exists that the merger/interaction is an important aspect in understanding the evolution of E+A galaxies.

Although we showed that E+A galaxies have 54% more companions than normal galaxies, our analysis also showed that less than 10% of E+A galaxies have companion galaxies. This result implies that the origin of a large fraction of E+A galaxies may not be a flyby interaction but a galaxy–galaxy merger (i.e., a parent galaxy engulfed its companion(s)).

Several caveats must be kept in mind. A merger/interaction can enhance star formation in galaxies. Lambas (2003) examined 1,258 galaxy pairs in the 100k public release of the 2dF galaxy survey and found that star formation in galaxy pairs is significantly enhanced over that of isolated galaxies for separations less than 36 kpc and velocity differences less than 100 km s^{-1} . In addition, Nikolic, Cullen & Alexander (2004) also investigated 12,492 galaxy pairs at projected separations of less than 300 kpc using the SDSS DR1, and reported that the mean specific star formation rate is significantly enhanced for projected separations of less than 30 kpc. E+A galaxies in our catalogue may evolve from these galaxies with violent star formation. Therefore, not every merging/interacting galaxy is an E+A galaxy. The fraction of E+A galaxies in the nearby Universe is too small ($\sim 0.02\%$; Goto 2005) for every merging/interacting galaxy to go through, even if the short timescale of the E+A phase ($\sim 1 \text{ Gyr}$) is considered. In our spectroscopic survey of E+A companion galaxies, some (true) companion galaxies are star-forming galaxies and other companion galaxies are passive (elliptical) galaxies. We found only one pair in this study in which a companion of an E+A galaxy is also an E+A galaxy. Therefore, another condition must exist for a merging/interacting galaxy to become an E+A.

Our work is based on local E+A galaxies. However, in

high-redshift cluster environments, the situation is different; E+A galaxies are much more numerous. Pioneering work was done by Dressler et al. (1999); Poggianti et al. (1999); Dressler et al. (2004), who found that E+A galaxies ($3\text{\AA} < H - E_{\text{EW}}$ and undetectable emission in D II) are significantly more common in 10 clusters at $0.37 < z < 0.56$ than in the field (21 \pm 2% compared to 6 \pm 3%). Later, Tran et al. (2003) found 7–13% of E+A galaxies in three high-redshift clusters at $z = 0.33; 0.58$ and 0.83 , claiming that $> 30\%$ of E+S0 members may have undergone the E+A phase if the effects of E+A downsizing and increasing E+A fraction as a function of redshift are considered (their selection criteria was $4\text{\AA} < \frac{H - E_{\text{EW}} + H - E_{\text{EW}}}{2}$ and $5\text{\AA} < \text{D II}E_{\text{EW}}$). In their search for field E+A galaxies amongst 800 spectra, Tran et al. (2004) measured the E+A fraction at $0.3 < z < 1$ to be $2.7\% \pm 1.1\%$, a value lower than that in galaxy clusters at comparable redshifts. When we refer to E+A galaxies, although we are looking at the same evolutionary stage of galaxies, it is important to keep in mind that the origin of E+A galaxies might be heterogeneous. For example, high-redshift cluster E+A galaxies may have a different physical origin from that of local field E+A galaxies.

We should also keep in mind that the magnitude range of our sample is limited to relatively bright magnitude ($-22.5 < M_r < -19.5$). It is expected that the fraction of E+A galaxies with a companion galaxy increases as we expand our spectroscopic survey of companion galaxies to fainter magnitude at $-19.5 < M_r$. It is also of importance to investigate a wide range of absolute magnitudes to reveal the luminosity dependence of the E+A phase. Magnitudes of the merger (major/minor) may have some effects in creating E+A galaxies. The time is right to consider deeper spectroscopic surveys of E+A companion galaxies with 4- to 8-m class telescopes.

Thus, our next goal is to clarify the evolution of E+A systems. For that, more detailed studies (e.g. Yagi & Goto 2006; Yagi, Goto & Hattori 2006; Goto 2007a) are needed. It is critical to investigate the spectroscopic properties of E+A companion galaxies and their dependence on the E+A properties. Revealing the effect of the local environment on E+A galaxies is also important future work.

ACKNOWLEDGEMENTS

We thank Diane Harmer, Daryl Willmarth, Judy Prosser and many KPNO staff members for much guidance and help in our preparations and observations. We are grateful to Dr. Hiroyasu Ando (NAOJ), Dr. Kunio Noguchi (NAOJ), Dr. Hiroshi Murakami (ISAS/JAXA), Dr. Takao Nakagawa (ISAS/JAXA) and M. S. Vijaya Kumar (TMU) for their support. We thank the anonymous referee for many insightful comments, which improved the paper significantly.

The research was supported by the Hayakawa Fund from the Astronomical Society of Japan.

Funding for the creation and distribution of the SDSS Archive has been provided by the Alfred P. Sloan Foundation, the Participating Institutions, the National Aeronautics and Space Administration, the National Science Foundation, the U.S. Department of Energy, the Japanese Monbukagakusho, and the Max Planck Society. The SDSS Web site is <http://www.sdss.org/>.

SDSS is managed by the Astrophysical Research Consortium (ARC) for the participating institutions, which are the University of Chicago, Fermilab, the Institute for Advanced Study, the Japan Participation Group, Johns Hopkins University, Los Alamos National Laboratory, the Max Planck Institute for Astronomy (MPIA),

the Max Planck Institute for Astrophysics (MPA), New Mexico State University, University of Pittsburgh, Princeton University, the United States Naval Observatory and the University of Washington.

This research made use of the NASA/IPAC Extragalactic Database (NED) operated by the Jet Propulsion Laboratory, California Institute of Technology, under contract with the National Aeronautics and Space Administration.

We thank Linux, XFree86, IRAF and other UNIX-related communities for the development of various useful software. This research made use of the Plamo Linux.

APPENDIX1: SPECTRA OF FAINT TARGETS OBSERVED WITH THE KPNO 2.1-M TELESCOPE

We actually observed two additional companion candidates as backup targets using the GoldCam at the KPNO. We show their spectra in Figure 5 and the target list is presented in Table 5. These backup targets do not have magnitudes that satisfy $M_r < -19.5$ for both the parent galaxy and companion candidates. In addition, the projection distance of target b2 is larger than 50 kpc. However, we found that these two candidates are also true companion galaxies. This result may contribute to future studies.

APPENDIX2: SPECTRA OF FORE/BACKGROUND GALAXIES OBSERVED AT KPNO 2.1-M TELESCOPE

We identified two fore/background galaxies around E+A galaxies by our KPNO observations. Results are shown in Figure 6 and Table 6.

REFERENCES

Abadi, M. G., Moore, B., & Bower, R. G. 1999, MNRAS, 308, 947
 Abazajian, K., et al. 2003, AJ, 126, 2081
 Abazajian, K., et al. 2004, AJ, 128, 502
 Abazajian, K., et al. 2005, AJ, 129, 1755
 Abraham, R. G., et al. 1996, ApJ, 471, 694
 Adelman-McCarthy, J., et al. 2006, ApJS, 162, 38
 Adelman-McCarthy, J., et al. 2007, ApJS, 172, 634
 Buyle, P., Michielsen, D., De Rijcke, S., Pisano, D. J., Dejonghe, H., and Freeman, K. 2006, ApJ, 649, 163
 Bartholomew, L. J., Rose, J. A., & Gaba, A. E. 2001, AJ, 122, 2913
 Barger, A. J., Aragon-Salamanca, A., Ellis, R. S., Couch, W. J., Smail, I., & Sharples, R. M. 1996, MNRAS, 279, 1
 Bekki, K., Shioya, Y., & Couch, W. J. 2001, ApJ, 547, L17
 Bekki, K., Couch, W. J., Shioya, Y., & Vazdekis, A. 2005, MNRAS, 359, 949
 Belloni, P., Bruzual, A. G., Thimm, G. J., & Roser, H.-J. 1995, A&A, 297, 61
 Bennett, C. L., et al. 2003, ApJS, 148, 1
 Blake, C., et al. 2004 MNRAS, 355, 713
 Blanton, M. R., et al. 2003, AJ, 125, 2348
 Broadhurst, T. J., Ellis, R. S., & Shanks, T. 1988, MNRAS, 235, 827
 Butcher, H., & Oemler, A. 1978, ApJ, 226, 559
 Caldwell, N., Rose, J. A., Sharples, R. M., Ellis, R. S., & Bower, R. G. 1993, AJ, 106, 473
 Caldwell, N., & Rose, J. A. 1997, AJ, 113, 492

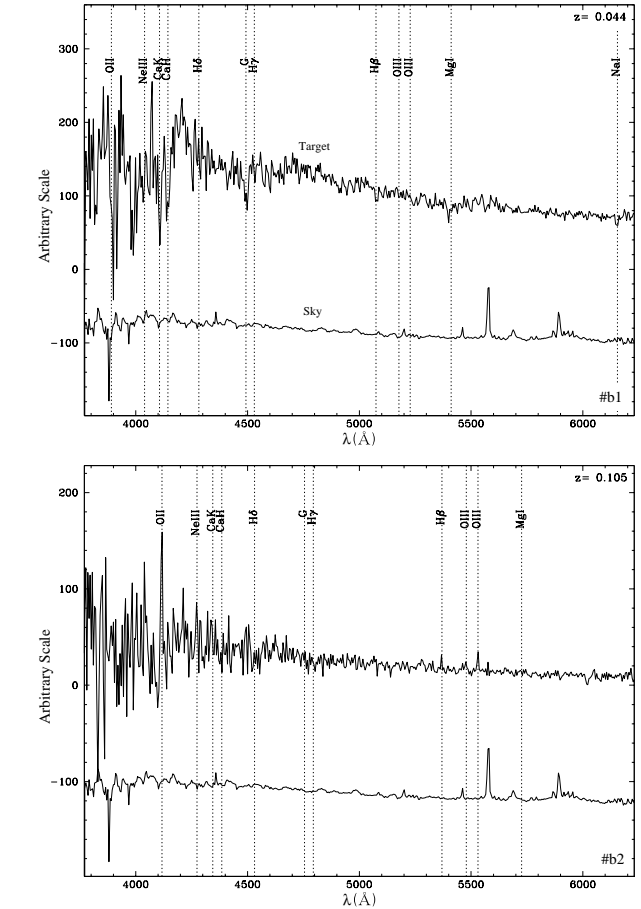
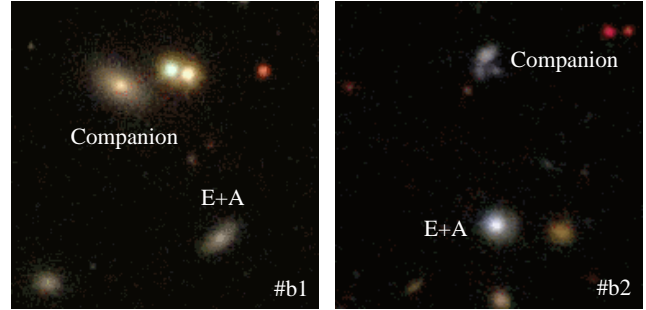


Figure 5. SDSS g,r,i -composite images and spectra of two new E+A's companions observed as backup targets with the KPNO 2.1-m telescope applying a 20Å binning. A sky spectrum in the observed data is shown at the bottom of each panel. Features to identify the redshift of candidates are C aK and C aH absorption lines (#b1) and [O III], H δ and [O III] emission lines (#b2), respectively.

Castander, F. J. et al. 2001, AJ, 121, 2331
 Chang, T., van Gorkom, J. H., Zabludoff, A. I., Zaritsky, D., & Mihos, J. C. 2001, AJ, 121, 1665
 Condon, J. J. 1992, ARA&A, 30, 575
 Couch, W. J., & Sharples, R. M. 1987, MNRAS, 229, 423
 Couch, W. J., Ellis, R. S., Sharples, R. M., & Smail, I. 1994, ApJ, 430, 121
 Couch, W. J., Barger, A. J., Smail, I., Ellis, R. S., & Sharples, R. M. 1998, ApJ, 497, 188
 Dressler, A. 1980, ApJ, 236, 351
 Dressler, A., & Gunn, J. E. 1983, ApJ, 270, 7

Table 5. List of backup targets with successful observation with the KPNO 2.1-m telescope.

Target	Observation	Exposure time	E+A galaxies							Companion galaxies							projection distance(kpc)
			R.A.	Dec.	r	M _r	z	H	EW	R.A.	Dec.	r	M _r	z	j	z j	
#b1	Sep.22,2005	30min.	2 01:15:37.59	+00:05:34.0	17.60	-18.80	0.044	4.50		01:15:39.20	+00:06:11.0	16.11	-20.29	0.044	0.000		37.42
#b2	Sep.24,2005	30min.	4 17:05:57.44	+63:00:55.7	16.66	-21.75	0.105	7.00		17:05:57.76	+63:01:33.2	18.50	-19.90	0.105	0.000		71.88

Table 6. List of fore/background galaxies with successful observation with the KPNO 2.1-m telescope.

Target	Observation	Exposure time	E+A galaxies							Fore/Background galaxies				
			R.A.	Dec.	r	M _r	z	H	EW	R.A.	Dec.	r	M _r	z
#f1	May.19,2007	20min.	3 11:22:33.75	+31:35:06.2	17.26	-21.34	0.114	4.54		11:22:35.57	+31:35:09.2	16.44	-22.29	0.121
#f2	May.20,2007	20min.	9 12:08:11.28	+40:21:51.2	16.42	-22.15	0.113	5.83		12:08:10.28	+40:21:47.0	17.93	-19.73	0.076

- Dressler, A., & Gunn, J. E. 1992, *ApJS*, 78, 1
- Dressler, A., Oemler, A. J., Sparks, W. B., & Lucas, R. A. 1994, *ApJ*, 435, L23
- Dressler, A., Smail, I., Poggianti, B. M., Butcher, H., Couch, W. J., Ellis, R. S., & Oemler, A. J. 1999, *ApJS*, 122, 51
- Dressler, A., Oemler, A. Jr., Poggianti, B. M., Smail, I., Trager, S., Shectman, S. A., Couch, W. J., Ellis, R. S. 2004, *ApJ*, 617, 867
- Ellingson, E., Lin, H., Yee, H. K. C., & Carlberg, R. G. 2001, *ApJ*, 547, 609
- Fabricant, D. G., McClintock, J. E., & Bautz, M. W. 1991, *ApJ*, 381, 33
- Farouki, R., & Shapiro, S. L. 1980, *ApJ*, 241, 928
- Fasano, G., Poggianti, B. M., Couch, W. J., Bettoni, D., Kjærgaard, P., & Moles, M. 2000, *ApJ*, 542, 673
- Fisher, D., Fabricant, D., Franx, M., & van Dokkum, P. 1998, *ApJ*, 498, 195
- Franx, M. 1993, *ApJ*, 407, L5
- Fujita, Y., & Nagashima, M. 1999, *ApJ*, 516, 619
- Fujita, Y. 2004, *PASJ*, 56, 29
- Fujita, Y., & Goto, T. 2004, *PASJ*, 56, 621
- Fukugita, M., Ichikawa, T., Gunn, J. E., Doi, M., Shimasaku, K., & Schneider, D. P. 1996, *AJ*, 111, 1748
- Goto, T., 2003, PhD Dissertation, University of Tokyo, astro-ph/0310196
- Goto, T. et al. 2003a, *PASJ*, 55, 739
- Goto, T. et al. 2003b, *PASJ*, 55, 771
- Goto, T., Yamauchi, C., Fujita, Y., Okamura, S., Sekiguchi, M., Smail, I., Bernardi, M., & Gomez, P. L. 2003c, *MNRAS*, 346, 601
- Goto, T. 2004, *A&A*, 427, 125
- Goto, T. 2005, *MNRAS*, 357, 937
- Goto, T. 2007, *MNRAS*, 377, 1222
- Goto, T. 2007, *MNRAS*, 381, 187
- Gunn, J. E., & Gott, J. R. I. 1972, *ApJ*, 176, 1
- Gunn, J. E., et al. 1998, *AJ*, 116, 3040
- Hogg, D. W., Schlegel, D. J., & Finkbeiner, D. P., & Gunn, J. E. 2001, *AJ*, 122, 2129
- Hogg, D. W., Masjedi, M., Berlind, A. A., Blanton, M. R., Quintero, A. D., & Brinkmann, J. 2006, *ApJ*, 650, 763
- Hopkins, A. M., et al. 2003, *ApJ*, 599, 971
- Kauffmann, G., et al. 2003, *MNRAS*, 341, 33
- Kennicutt, R. C. 1998, *ARA&A*, 36 189
- Kent, S. M. 1981, *ApJ*, 245, 805
- Kodama, T. & Bower, R. G. 2001, *MNRAS*, 321, 18
- Komatsu, E., et al. 2008, *ApJS*, submitted
- Lambas, D. G., Tissera, P. B., Sol Alonso, M., & Coldwell, G. 2003, *MNRAS*, 346, 1189
- Lavery, R. J. & Henry, J. P. 1986, *ApJ*, 304, L5
- Lavery, R. J. & Henry, J. P. 1988, *ApJ*, 330, 596
- Liu, C. T., & Kennicutt, R. C. 1995a, *ApJS*, 100, 325
- Liu, C. T., & Kennicutt, R. C. 1995b, *ApJ*, 450, 547
- MacLarn, I., Ellis, R. S., & Couch, W. J. 1988, *MNRAS*, 230, 249
- Margoniner V. E., de Carvalho R. R., Gal R. R., Djorgovski S. G. 2001, *ApJ*, 548, L143
- Miller, N. A., & Owen, F. N. 2001, *ApJ*, 554, L25
- Morris, S. J., Hutchings, J. B., Carlberg, R. G., Yee, H. K. C., Ellingson, E., Balogh, M. L., Abraham, R. G., & Smecker-Hane, T. A. 1998, *ApJ*, 507, 84
- Newberry, M. V., Boroson, T. A., & Kirshner, R. P. 1990, *ApJ*, 350, 585
- Nikolic, B., Cullen, H., & Alexander, P. 2004, *MNRAS*, 355, 874
- Norton, S. A., Gebhardt, K., Zabludoff, A. I., & Zaritsky, D. 2001, *ApJ*, 557, 150
- Oegerle, W. R., Hill, J. M., & Hoessel, J. G. 1991, *ApJ*, 381, L9
- Oemler, A. J., Dressler, A., & Butcher, H. R. 1997, *ApJ*, 474, 561
- Pier, J. R., Munn, J. A., Hindsley, R. B., Hennessy, G. S., Kent, S. M., Lupton, R. H., & Ivezić, Z. 2003, *AJ*, 125, 1559
- Poggianti, B. M., Smail, I., Dressler, Alan., Couch, W. J., Barger, A. J., Butcher, H., Ellis, R. S., & Oemler, A. Jr. 1999, *ApJ*, 518, 576
- Poggianti, B. M., & Wu, H. 2000, *ApJ*, 529, 157
- Poposo, P., Biviano, A., Romaniello, M., & Böhringer, H. 2007, *A&A*, 461, 411
- Postman M., Geller M. J. 1984, *ApJ*, 281, 95
- Postman M., et al. 2005, *ApJ*, 623, 721
- Quilis, V., Moore, B., & Bower, R. 2000, *Sci*, 288, 1617
- Quintero, A. D., et al. 2004, *ApJ*, 602, 190
- Rakos, K. D., & Schombert, J. M. 1995, *ApJ*, 439, 47
- Rose, J. A., Gaba, A. E., Caldwell, N., & Chaboyer, B. 2001, *AJ*, 121, 793
- Schweizer, F. 1982, *ApJ*, 252, 455
- Schweizer, F. 1996, *AJ*, 111, 109
- Sharples, R. M., Ellis, R. S., Couch, W. J., & Gray, P. M. 1985, *MNRAS*, 212, 687
- Smail, I., Morrison, G., Gray, M. E., Owen, F. N., Ivison, R. J., Kneib, J.-P., & Ellis, R. S. 1999, *ApJ*, 525, 609

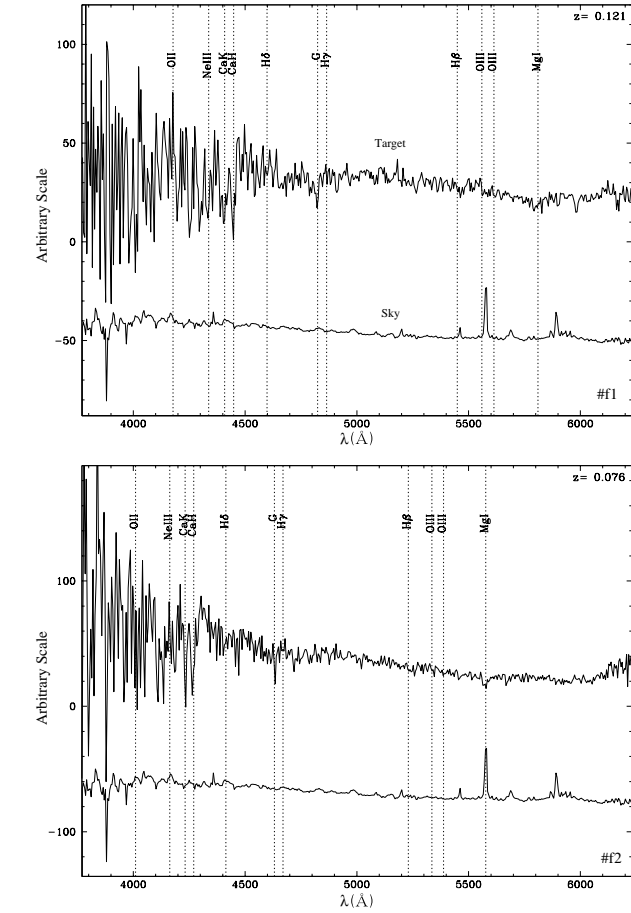
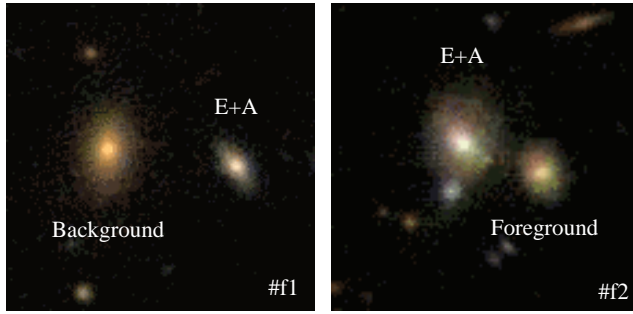


Figure 6. SDSS g,r,i -composite images and spectra of two fore/background galaxies taken with the KPNO 2.1-m telescope applying a 20Å binning. A sky spectrum in the observed data is shown at the bottom of each panel. Features to identify the redshift of candidates are C aK and C aH absorption lines.

- D. D., & Magee, D. 2004, *ApJ*, 609, 683
 Yagi, M., & Goto, T. 2006, *AJ*, 131, 2050
 Yagi, M., Goto, T., & Hattori, T. 2006, *ApJ*, 642, 152
 Yamauchi, C., & Goto, T. 2005, *MNRAS*, 359, 1557
 Yang, Y., Zabludoff, D., Zaritsky, D., Lauer, T., & Mihos, J. C. 2004, *ApJ*, 607, 258
 Yasuda, N., et al. 2001, *AJ*, 122, 1104
 York, D. G., et al. 2000, *AJ*, 120, 1579

- Smith, J. A., et al. 2002, *AJ*, 123, 2121
 Smith, G. P., Treu, T., Ellis, R. S., Moran, S. M., & Dressler, A. 2005, *ApJ*, 620, 78S
 Spitzer, L. J., & Baade, W. 1951, *ApJ*, 113, 413
 Stoughton, C., et al. 2002, *AJ*, 123, 485
 Strauss, M. A. et al. 2002, *AJ*, 124, 1810
 Tanaka, M., Goto, T., Shimasaku, K., Okamura, S., Shimasaku, K., & Brinkmann, J. 2004, *ApJ*, 128, 2677
 Tran, K. H., Franx, M., Illingworth, G., Kelson, D. D., & van Dokkum, P. 2003, *ApJ*, 599, 865
 Tran, K. H., Franx, M., Illingworth, G., van Dokkum, P., Kelson,